JOURNAL OF MATERIALS SCIENCE 28 (1993) 4489–4496

Prediction of fibre strength at the critical length: a simulation theory and experimental verification for bimodally distributed carbon fibre strengths

TAEHWAN JUNG, R. V. SUBRAMANIAN, V. S. MANORANJAN*
*Department of Mechanical and Materials Engineering, and *Department of Mathematics, Washington State University, Pullman, WA 99164, USA*

A computer simulation model of fragment distribution with respect to the fibre strength in a single-filament composite test is developed using the bimodal Weibull statistics. The predictions of the theory are examined with experimental results for AU carbon fibres coated by zirconium-*n*-propoxide or a zircoaluminate complex. Weibull analysis reveals a bimodal distribution of fibre strengths, in which the fractions of low- and high-strength populations vary with gauge length. It is seen that the simulation results are in good agreement with experimental data if the best fit model of strength distribution is applied. Thus, the use of a bimodal distribution term in the simulation theory yields a predicted strength at the critical length which is in good agreement with the results of extrapolation of experimental data, while the unimodal distribution term leads to overestimation of the strength.

1. Introduction

Carbon fibre-reinforced composite materials have become very attractive structural materials in many branches of aerospace and other industries because of their light weight combined with high strength and modulus. In the fibre-reinforced composite system, one of the most important controlling factors is the interfacial property which relates to the capacity of stress transfer from the matrix to the reinforcing fibre. Although the high strength of a composite is due to strong bonding between the fibre and the matrix, a low interfacial bonding strength due to a relatively weak bonding improves the fracture toughness of the composite. For this important reason, many investigations are devoted to research characterizing the interfacial behaviour in the composite system.

There are various techniques to characterize interfacial shear strength between the fibre and matrix [1]. Among them, the single-filament composite (SFC) test is frequently used to study interfacial shear strength in the composite [2–6]. This test was originally used to investigate the interfacial shear strength in the fibre/metal composite system by Kelly and Tyson [2]. The method is based on force balance when tensile stress is transferred to the interface parallel to the fibre axis. Assuming that the matrix is perfectly plastic, the shear stress, τ, is a constant along the critical length, l_c. Therefore, the relationship between fibre strength, s_f, and the shear stress at the critical length is

$$\tau = \frac{S_f . d}{2 l_c} \quad (1)$$

where d is the diameter of the fibre. In Equation 1, the critical length and diameter of the fibre can be obtained from the SFC test. However, it is impractical to measure directly the fibre strength at the critical length, because the critical length is too short for measurement by conventional tensile tests. It is the usual practice to extrapolate tensile strength data at measurable gauge lengths to the critical length using an approximately linear relationship between the fibre strength and the logarithm of gauge length [7].

Recently, a probability model and a Monte Carlo method were used to predict a realistic value for the interfacial strength between the fibre and the matrix [8, 9]. A notable new development [10] is the formulation of an exact theory to express the relationship between the fibre fragmentation and the underlying fibre statistical strength in the SFC test. These simulation theories are based on the unimodal Weibull distribution for the fibre fracture. Generally, the unimodal Weibull distribution does not fit well the experimental data because of the presence of various kinds of imperfections such as surface defects, and internal defects including misoriented crystallites and undetectable defects [11–14]. But, the Weibull distribution curve predicted from the bimodal distribution is known to be a better fit with the experimental data than the unimodal distribution [15, 16]. For this reason, the unimodal distribution model used in simulation theories needs to be modified to a multimodal distribution model if the fibre strength data reveal more than one type of defect.

The objective of this paper is to obtain the fibre

0022–2461

strength at the critical length using the exact theory developed by Curtin [10], but with bimodal Weibull statistics, and then compare the strength obtained by simulation with the strength obtained by extrapolating the experimental data. The fibres investigated are AU carbon fibres coated in the laboratory by zirconium-*n*-propoxide (ZNP) or zircoaluminate complex (AZ). The choice of these coated fibres for the study is related to the potential importance of zirconia coating in interphase modification of graphite fibre-reinforced metal matrix composites [17].

2. Analysis of the fibre strength

The strength of a brittle fibre is often analysed by the Weibull statistical model which is based on the weakest link theory. According to this theory, the most severe defect among all defects existing on the fibre dominates the fibre failure process [18]. So, the unimodal cumulative Weibull distribution for the fibre strength in which only one defect controls the fibre failure process is

$$F(s) = 1 - \exp\left[-\left(\frac{s}{s_0}\right)^m\right] \quad (2)$$

where m and s_0 are the shape parameter and the scale parameter, respectively. The parameters m and s_0 can be obtained by the maximum likelihood method of estimation as follows [19]

$$\frac{1}{m} + \frac{1}{n}\sum_{i=1}^{n}\ln s_i - \frac{\sum_{i=1}^{n} s_i^m \ln s_i}{\sum_{i=1}^{n} s_i^m} = 0 \quad (3)$$

$$s_0 = \left(\frac{1}{n}\sum_{i=1}^{n} s_i^m\right)^{1/m} \quad (4)$$

where n is the sample size and s_i the fibre strength of the ith order, where the strengths are placed in ascending order, s_1 being the lowest strength and s_n the highest strength. The shape parameter, m, can be found by an iterative procedure using Equation 3, and if m is known, s_0 can be determined easily from Equation 4.

However, the unimodal distribution function based on the single defect model does not fit well the experimental data if there exist defects of various kinds rather than of only one kind. Therefore, a multimodal distribution function is required if the defect types are more than one. The cumulative bimodal Weibull distribution function based on the presence of two kinds of defect is described as follows [14]

$$F(s) = 1 - \left\{p\exp\left[-\left(\frac{s}{s_{01}}\right)^{m_1}\right] + q\exp\left[-\left(\frac{s}{s_{02}}\right)^{m_2}\right]\right\} \quad (5)$$

$$p + q = 1 \quad (6)$$

where p and q are portions of low-strength and high-strength populations, respectively, and m_1, m_2, S_{01} and S_{02} are the shape and scale factors for low-strength and high-strength portions, respectively. The probability density function of the Weibull distribution can be obtained by differentiating the cumulative distribution function. Generally, the low-strength portion is generated by defects caused by surface damage during handling and the high-strength portion is due to the internal defects [20].

3. Simulation model of fragmentation versus fibre strength

In order to predict the fibre strength at the critical length in the SFC test, various methods are used such as Weibull statistics or extrapolation of experimental strength data at different gauge lengths. However, these methods cannot give information regarding the relationship between the fibre fragmentation and fibre strength while the fibre is broken successively during elongation of an SFC specimen. The relationships of the number of breaks, N, and the length of remaining fibre, L, with respect to the fibre strength, s, which was proposed by Curtin [10], are

$$\frac{dL}{ds} = -N\delta P(\delta;\eta)\frac{d\delta}{ds} \quad (7)$$

$$\frac{dN}{ds} = -NP(\delta;\eta)\frac{d\delta}{ds} + f(s, L^*) \quad (8)$$

$$L^* = N\int_{2\delta}^{\infty}(x - 2\delta)\,P(x;\eta)\,dx \quad (9)$$

where δ is the recovery length which is equal to $l_c/2$, and $\eta = \delta N/L$. $P(\delta;\eta)$ is the unique strength fragment distribution

$$P(\delta;\eta) = \frac{2}{\eta\delta}\int_0^{\eta}\psi(\eta')\,d\eta' \quad (10)$$

with

$$\psi(\eta) = \frac{\exp(-2\gamma)}{\eta^* - \eta} \quad (11)$$

where γ is Euler's constant ($= 0.5772$) and η^* is 0.7476 [10].

The strength distribution term in Equation 8 based on the power series of Weibull distribution for the fibre length, L, is

$$f(s, L^*) = \frac{L^* m}{L_0 s_0}\left(\frac{s}{s_0}\right)^{m-1} \quad (12)$$

However, this strength distribution term would not be correct if the strength distribution in actual experiments shows multiple modes. Therefore, the strength distribution term needs to be modified to the multimodal term if necessary.

Such a modified form of Equation 12 for bimodal distribution is

$$f(s, L^*) = \frac{L^*}{L_0}\left[p\frac{m_1}{s_{01}}\left(\frac{s}{s_{01}}\right)^{m_1-1} + q\frac{m_2}{s_{02}}\left(\frac{s}{s_{02}}\right)^{m_2-1}\right] \quad (13)$$

The relationship between the fibre strength and fragmentation can be predicted by integrating Equations 7

and 8 with strength distribution terms from either Equation 12 or 13. The differential equations can be solved easily using a numerical method with an iterative procedure. In this paper, the simulation is performed with Advanced Continuous Simulation Language (ACSL). From the simulation results, the fibre strength when there is a maximum number of breaks can be considered as the fibre strength at the critical length.

4. Experimental procedure

SFC test specimens were prepared in order to evaluate and compare the simulation model with the experimental data. As a reinforcing fibre, Hercules high-modulus untreated carbon fibre (AU type fibre) was used. The epoxy matrix resin diluted with 10 wt % phenyl glycidyl ether (Aldrich Chemical Co.) was diglycidyl ether of bisphenol-A (Epon 828, Shell Chemical Co.) and cured at 150 °C with 14.5 p.h.r. *m*-phenylenediamine (Aldrich Chemical Co.). Before embedding in an epoxy matrix, the fibres were coated by zirconia or zircoaluminate. As coating materials, zirconium-*n*-propoxide (Alpha Products Co.) and zircoaluminate solution (Cavco Mod M-1, Cavedon Chemical Co., Inc.) were prepared. The zirconium-*n*-propoxide was mixed with ethyl acetoacetate at one-to-one molar ratio in order to reduce the reaction rate with moisture in air. The zircoaluminate (AZ) solution and the stabilized zirconium-*n*-propoxide (ZNP) solution were diluted by ethanol with a volume ratio of 1/20. The solutions were stirred for 4 h and stored in plastic containers. The AU fibres were fixed on stainless steel frames with aluminium tapes and dipped into the solutions. The frames were withdrawn vertically at a speed of 20 cm min^{-1}. These coated fibres were hydrolysed in hot steam (60 °C) for 15 min and dried at 180 °C for 30 min. The SFC samples were made by the method described elsewhere [4].

The tensile strengths of individual fibres mounted on paper frames were measured using a tensile testing machine with the crosshead speed of 1 mm min^{-1}. The load readings were recorded on a chart by an x–y recorder. About 40 fibre specimens were tested for each test at a particular gauge length: gauge lengths of 3, 6.5, 10 and 22 mm were chosen in these experiments. The tensile strength in each test was analysed by both unimodal and bimodal Weibull statistics.

5. Results and discussion

5.1. Analysis of strength distribution

From the tensile strength tests of the AU fibre with different coatings, the strength distributions of the different fibres were analysed by Weibull statistics. Fig. 1 shows the cumulative strength distribution of the fibre coated by the stabilized ZNP solution at 6.5 mm gauge length. The experimental strength data were estimated from $F(s) = i/(N + 1)$, where N is the total number of samples tested and i is the ith number in ascendingly ordered strength data. It is easily seen that the bimodal distribution curve (Fig. 1b) is a better fit to the experimental data than the unimodal distribution curve (Fig. 1a). The Weibull parameters for bimodal distribution are presented in Tables I and II for the two types of fibre tested. The results indicate the presence of two kinds of defect governing the strength of the fibre.

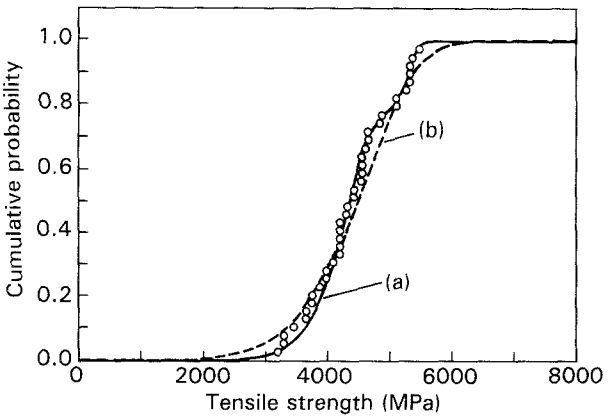

Figure 1 Cumulative Weibull distribution curves, (a) unimodal and (b) bimodal for the strength of ZNP-coated AU fibres (gauge length 6.5 mm).

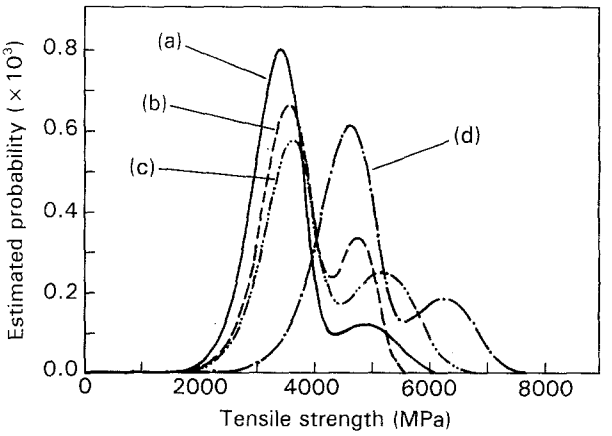

Figure 2 Bimodal Weibull distribution of AZ-coated AU fibres, gauge lengths: (a) 22 mm, (b) 10 mm, (c) 6.5 mm and (d) 3 mm.

Fig. 2 shows estimated distribution curves of the tensile strengths for the AU fibre coated by AZ solution, at different gauge lengths. The low-strength population due to surface flaws on the fibre is decreased and the high-strength population caused by internal defects is increased as the gauge length is reduced. At 3 mm gauge length, the lowest strength population due to surface damage has disappeared. However, the strength distribution still shows bimodality because of the appearance of a new population at the highest strength region. From the result, it is noted that the AU fibre coated by AZ solution has three kinds of defect and at least two of these defects controlled the strength of the fibre at any one gauge length used in the experiment.

The Weibull plots of tensile strengths at different gauge lengths for the AU fibre coated by ZNP solution are shown in Fig. 3. The trends of the distribution curves are similar to the plots in Fig. 2. The lowest strength population is eliminated at the lowest gauge

TABLE I Simulation results using bimodal Weibull distribution for AZ-coated AU fibre at different gauge lengths, L

L (mm)	Population[a]	Weibull parameter		Strength[b] (MPa)	Number of fragments[b]
		m	S_0(MPa)		
22	31/88	9.03	3477	6360	55
	7/38	9.02	4990		
10	26/39	9.35	3607	6060	56
	13/39	13.27	4805		
6.5	23/40	9.17	3653	6210	56
	17/40	8.37	5272		
3	27/38	10.48	4670	6650	57
	11/38	10.93	6324		

[a] Ratios of low- and high-strength populations.
[b] Estimated values.

TABLE II Simulation results using bimodal Weibull distribution for ZNP-coated AU fibre at different gauge lengths, L

L (mm)	Population[a]	Weibull parameter		Strength[b] (MPa)	Number of fragments[b]
		m	S_0(MPa)		
22	22/40	12.47	3374	5370	43
	18/40	10.02	4752		
10	9/40	10.7	3229	5510	42
	31/40	11.26	4708		
6.5	30/38	11.2	4355	6070	46
	8/38	51.74	5344		
3	16/39	13.43	4226	5750	44
	23/39	14.26	5691		

[a] Ratios of low- and high-strength populations.
[b] Estimated values.

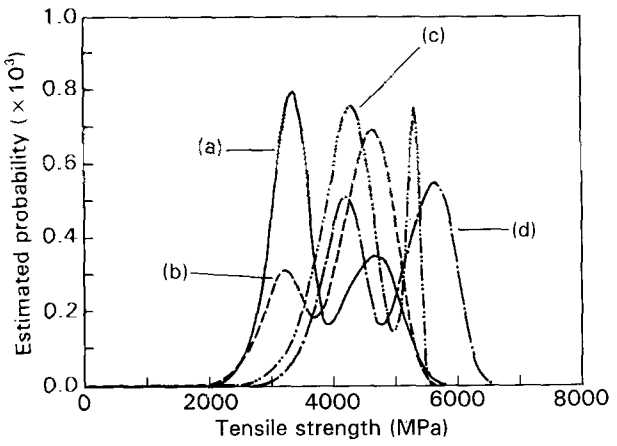

Figure 3 Bimodal Weibull distribution of ZNP-coated AU fibres, gauge lengths: (a) 22 mm, (b) 10 mm, (c) 6.5 mm and (d) 3 mm.

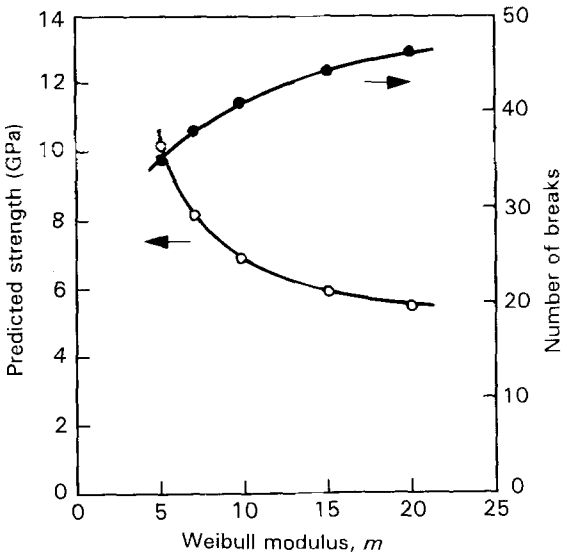

Figure 4 Predicted dependence, on the Weibull modulus, of (○) fibre strength and (●) number of breaks in an SFC specimen, using unimodal distribution (gauge length 22 mm, scale parameter 4142 MPa).

length, and a new population appears at the high end. However, the low-strength portion in this case, particularly at gauge lengths 10 mm and lower, is smaller than that in Fig. 2. The severity and distribution of surface flaws of the fibre seem to have been altered by the application of a different coating.

5.2. Simulation of fragment distribution

In this section, computer simulation results of the model with Equations 7 and 8 are presented. Fig. 4 shows the predicted values for the maximum strengths of the fibre, and the maximum number of breaks as a function of Weibull modulus, m. Unimodal Weibull distribution (Equation 12) is used, with gauge length

at 22 mm and scale parameter, s_0, fixed at 4142 MPa. It is clear from the figure that the predicted maximum strength of the fibre, which is considered the fibre strength at the critical length, decreases as the Weibull modulus increases. But, the maximum number of fibre breaks also increases slightly as the Weibull modulus is increased. This result emphasizes that the strength distribution term in Equation 8 has a strong influence on the fragment distribution. Therefore, the best fit model of the strength distribution is required in order to obtain reasonable strength predictions from the equations.

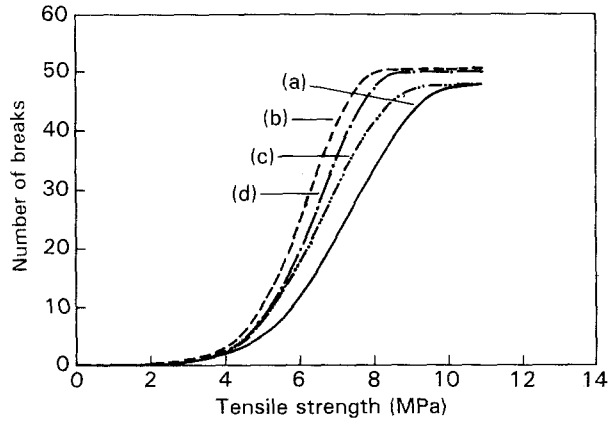

Figure 5 Predicted cumulative number of fibre breaks in SFC specimens at increasing breaking strengths for AZ-coated AU fibres using unimodal distribution of fibre strengths at gauge lengths (a) 22 mm, (b) 10 mm, (c) 6.5 mm and (d) 3 mm.

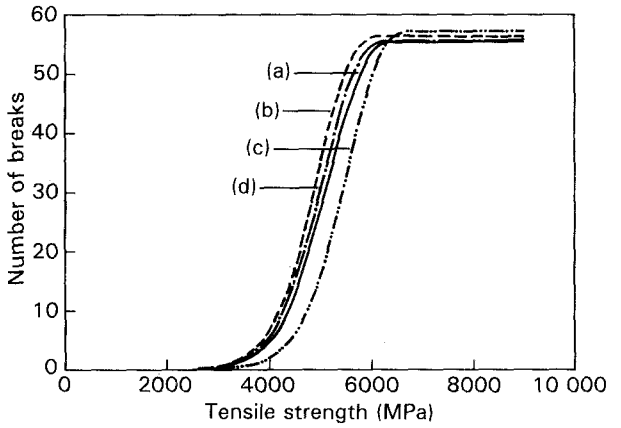

Figure 6 Predicted cumulative number of fibre breaks in SFC specimens at increasing breaking strengths for AZ-coated AU fibres using bimodal distribution of fibre strengths at gauge lengths (a) 22 mm, (b) 10 mm, (c) 6.5 mm and (d) 3 mm.

This is further examined in results presented in Figs 5 and 6 for predicted cumulative fibre fragment distributions as functions of the measured strength at different gauge lengths for the AU fibre coated by AZ solution. These distribution curves are obtained by integrating Equations 7 and 8 with unimodal (Fig. 5) and bimodal (Fig. 6) Weibull statistics. Comparing these figures, it is seen that in Fig. 5 the fragment distribution curves for different gauge lengths show more deviation between themselves in the slope and in the maximum number of breaks, than in Fig. 6. The slopes of the fragment distribution curves in Fig. 5 increase with increase in the Weibull modulus, m, at different gauge lengths (Table III). Here again is the clear indication that the fibre fragment distribution obtained by simulation is influenced by the fibre strength distribution. Also, the bimodal distribution is found to be a better fit to experimental data than the unimodal distribution. Consequently, simulation results at any tested gauge length can be easily obtained using bimodal distribution.

Consistent with these observations, the same trends were observed for the case of AU fibre coated by ZNP solution. As before, the cumulative fibre fragment distributions, as functions of fibre strength, were predicted by numerically integrating Equations 7 and 8 using the experimental strength data. In this case also, less deviation was observed among the data obtained from different gauge lengths, when the bimodal distribution term is used in Equation 8, and the slopes are also steeper, than when the unimodal distribution term is used. Furthermore, the distribution curves fall close to each other when the Weibull moduli of the strength data are about the same at gauge lengths 10 and 3 mm (Table IV). From these results, it is clear that the fragment distribution is influenced by the Weibull modulus of the fibre strength.

5.3. Fibre strength prediction at short gauge lengths

The predicted fibre strengths at the critical length estimated by numerical simulation for the AU fibre coated by AZ and ZNP solutions are shown in Figs 7 and 8, respectively. All data shown in Figs 7 and 8 are based on tensile strength tests of single fibres. The mean tensile strength of the fibres at each of four different gauge lengths is plotted in the figures, and the straight line is obtained using linear regression of the strength data with respect to the logarithm of gauge length. Also plotted are the maximum fibre strengths

TABLE III Simulation results using unimodal Weibull distribution for AZ-coated AU fibre at different gauge lengths, L

L	Size of	Weibull parameter		Strength[a]	Number of
(mm)	samples	m	S_0(MPa)	(MPa)	fragments[a]
22	38	4.81	3857	10 470	48
10	39	5.81	4116	8 420	50
6.5	40	4.75	4485	9 520	47
3	38	5.7	5302	8 860	50

[a] Estimated values.

TABLE IV Simulation results using unimodal Weibull distribution for ZNP-coated AU fibre at different gauge lengths, L

L	Size of	Weibull parameter		Strength[a]	Number of
(mm)	samples	m	S_0(MPa)	(MPa)	fragments[a]
22	40	5.48	4142	9550	36
10	40	7.23	4485	7790	38
6.5	38	8.01	4664	7350	39
3	39	7.09	5250	7760	38

[a] Estimated values.

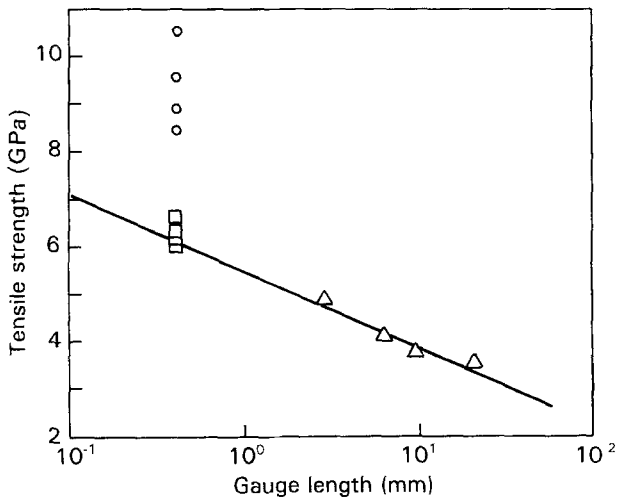

Figure 7 Predicted fibre strengths at the critical length (0.41 mm) using (○) unimodal distribution and (□) bimodal distribution of (△) experimental data at gauge lengths 22, 10, 6.5 and 3 mm for AZ-coated AU fibres.

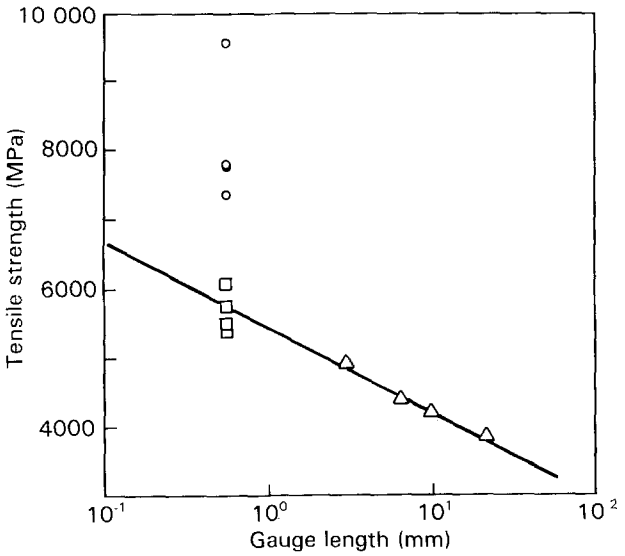

Figure 8 Predicted fibre strengths at the critical length (0.553 mm) using (○) unimodal distribution and (□) bimodal distribution of (△) experimental data at gauge lengths 22, 10, 6.5 and 3 mm for ZNP-coated AU fibres.

at the critical lengths 0.41 mm (Fig. 7) and 0.553 mm (Fig. 8), estimated by numerical simulation using the bimodal distribution model with different gauge lengths. For comparison, the maximum strengths estimated using the unimodal distribution model are also shown. The fibre strengths obtained using the unimodal distribution model give overestimated strengths compared to the extrapolated strength at the critical length using the experimental data. This illustrates clearly that, in the case of fibres used in the present study, the unimodal distribution model is not a good fit to the experimental data. On the other hand, the fibre strengths estimated using the bimodal distribution model are in good agreement with the extrapolated strength. It is also clear from these observations that Equations 7 and 8 are strongly dependent on strength distribution, and simulation results will be in good agreement with experimental data if the best fit model of strength distribution is applied.

The simulation results using bimodal Weibull distribution for AZ- and ZNP-coated fibres with different gauge lengths are included in Tables I and II, respectively. The values of the fibre strength at the critical length, estimated from data for each gauge length, are similar. The corresponding simulation results using unimodal distribution are shown in Tables III and IV. Here the estimated strengths show large differences through the gauge lengths tested. It is evident that the strength at the critical length could be predicted by the simulation model using bimodal strength distribution, thus obviating the need for extrapolation of data for many different gauge lengths. It should be noted that a simulation model using the unimodal strength distribution can also be a valid instance, though not in our case. Obviously, the choice of the appropriate model would be based on the experimental data for strength distribution.

It is also of interest to follow the course of fibre fragmentation in SFC specimens. Fig. 9 illustrates the

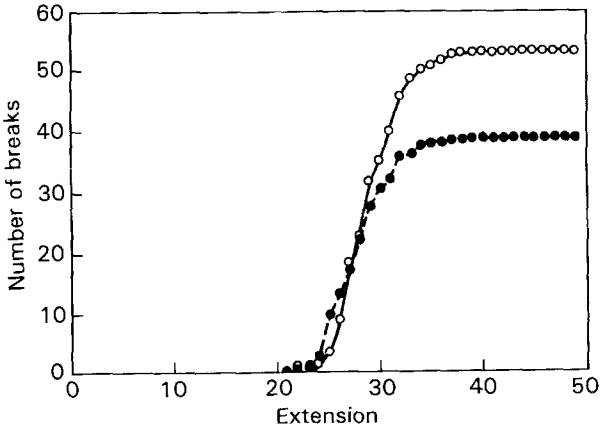

Figure 9 Variation of average number of fibre breaks with extension of SFC specimens of AU fibre coated by (○) AZ and (●) ZNP.

TABLE V Weibull modulus for the fragment distribution of ZNP- and AZ-coated AU fibres in SFC specimens, experimental values and simulations at different gauge lengths, L

	L(mm)	Weibull modulus (m)			
		ZNP coating		AZ coating	
		Unimodal	Bimodal	Unimodal	Bimodal
Simulation	22	5.73	11.99	5.08	9.02
	10	7.39	10.54	6.11	9.18
	6.5	8.08	12.62	5.13	9.47
	3	7.24	12.95	5.99	10.27
Experiment		9.76		11.07	

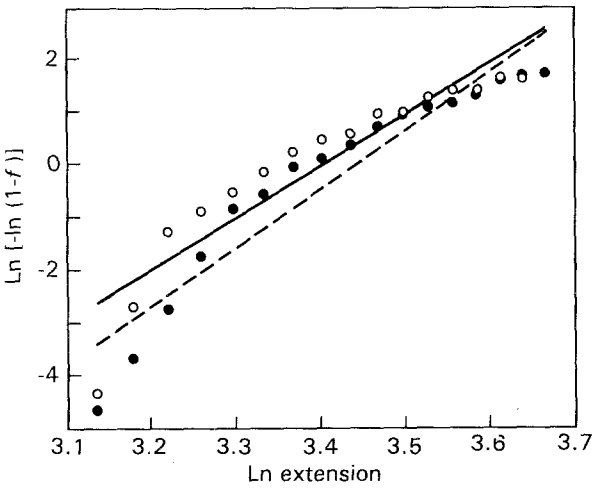

Figure 10 Weibull plot of fibre fragmentation in SFC specimens of AU fibre coated by (●) AZ and (○) ZNP.

average number of fibre breaks plotted as a function of extension of the SFC sample for the fibres with different coatings. The number of breaks in the fibre are seen to increase as the elongation of the specimen increases. The mean of the maximum number of breaks in the SFC specimens of the fibre coated by AZ solution is 53 and that for the fibre coated by ZNP solution is 39. Fig. 10 shows the plots of $\ln[-\ln(1-f)]$ as a function of ln (extension) for both fibres in the SFC tests. The cumulative probability of the fibre breaks is estimated with $f = N_i/N_T$ where N_T is the total number of fibre breaks and N_i is the number of breaks at a certain extension. The experimental data show some deviation from the estimated lines. This is most likely due to debonding of the fibre during extension. When debonding starts, there is no linear relationship between the stress transferred to the fibre and the extension of the SFC specimen.

Table V presents the Weibull modulus, m, for the fragment distribution of the AU fibre with different coatings in the SFC test along with simulations for different gauge lengths. The modulus values for different gauge lengths obtained from simulations using the bimodal distribution model are less deviant among themselves for different gauge lengths than those obtained using the unimodal distribution model.

6. Conclusions

The exact theory of fibre fragmentation in SFC specimens [10] can be suitably modified to take into account the bimodal distribution of fibre strength, which usually occurs with carbon fibres. The statistical factors are thus more completely represented in the modified theory.

The application of the theory is illustrated for two differently coated AU fibres, one by AZ and another by ZNP solutions both of which show bimodally distributed fibre strengths, and a strong dependence of strength population fractions on gauge length. For such cases, it is demonstrated that simulation using the bimodal strength distribution term instead of a unimodal term yields better agreement with experimental data, through all gauge lengths studied.

The important conclusion is that the fibre strength, at the critical length, which is impossible to measure with currently available experimental methods, can be predicted accurately using this simulation theory. Not only is the prediction reasonably accurate compared to extrapolation of experimental data, but simulation also eliminates the need for extensive data collection at different gauge lengths, which would be required for extrapolation.

It should also be pointed out that, where the fibre strength is bimodally distributed, the use of unimodal distribution in the simulation theory will overestimate the strength at the critical length, which would be undesirable for practical considerations.

References

1. M. NARKIS, E. J. H. CHEN and R. B. PIPES, *Polym. Compos.* **9** (1988) 245.
2. A. KELLY and N. R. TYSON, *J. Mech. Phys. Solids* **13** (1965) 329.
3. L. T. DRZAL, M. J. RICH and P. F. LLOYD, *J. Adhes.* **16** (1982) 1.
4. A. S. CRASTO, S. H. OWN and R. V. SUBRAMANIAN, *Polym. Compos.* **9** (1988) 78.
5. A. N. NETRAVALI, R. B. HENSTENBURG, S. L. PHOENIX and P. SCHWARTZ, *ibid.* **10** (1989) 226.
6. W. D. BASCOM and R. M. JENSEN, *J. Adhes.* **19** (1986) 219.
7. J. D. H. HUGHES, *J. Phys. D Appl. Phys.* **20** (1987) 276.
8. R. B. HENSTENBURG and S. L. PHOENIX, *Polym. Compos.* **10** (1989) 389.
9. W. A. FRASER, F. H. ANCKER, A. T. DIBENEDETTO and B. ELBIRLI, *ibid.* **4** (1983) 238.

10. W. A. CURTIN, *J. Mater. Sci.* **26** (1991) 5239.
11. D. J. JOHNSON, *J. Phys. D Appl. Phys.* **20** (1987) 386.
12. J. W. HITCHON and D. C. PHILLIPS, *Fibre Sci. Technol.* **12** (1979) 217.
13. S. C. BENNETT, D. J. JOHNSON and W. JOHNSON, *J. Mater. Sci.* **18** (1983) 3337.
14. S. H. OWN, R. V. SUBRAMANIAN and S. C. SAUNDERS, *ibid.* **21** (1986) 3912.
15. K. GODA and H. FUKUNADA, *ibid.* **21** (1986) 4475.
16. C. P. BEETZ Jr, *Fibre Sci. Technol.* **16** (1982) 45.
17. R. V. SUBRAMANIAN and E. A. NYBERG, *J. Mater. Res.* **7** (1992) 677.
18. W. WEIBULL, *J. Appl. Mech.* **18** (1951) 293.
19. S. N. PATENKAR, *J. Mater. Sci. Lett.* **10** (1991) 1176.
20. J. B. DONNET and R. C. BANSAL, "Carbon Fibres" (Marcel Dekker, New York, 1990) p. 289.

Received 2 June 1992
and accepted 3 February 1993